E-Space

Steven Bevacqua, EE, Spencer Pietryka, EE, Jonathan Scharf, EE

***Abstract*—The current implementation of wireless power transfer uses inductive power transfer, involving strongly coupled coils and high efficiency, close range transfer. This technology only works with ranges less than a few centimeters, and the coils must be orientated correctly to affect efficient power transfer. A different technology known as Magnetic Resonant Power Transfer has emerged that promises mid range, yet still high efficiency power transfer. The transmitting and receiving coils are loosely coupled, meaning the distance between them and their relative orientation is much more flexible, but resonate at a fixed frequency that still facilitates efficient transfer between them. Using this technology we are implementing a wireless power transfer system to charge a wireless phone at farther ranges than is possible with inductive technology.**

I. Introduction

Since the 1970's, transistor count and computing speed has followed Moore's law, doubling every 18 months. However in that time, battery technology has lagged far behind, with energy density only doubling between 1980 and 2010 [1]. This and the proliferation of devices including smartphones, tablets, and laptops, has led to a major problem in keeping devices charged while living an increasingly mobile life. Public locations like airports, parks, and college campuses include built-in charging stations for mobile devices or banks of outlets in their designs. The need for charging cables and ports is also an inherent weakness in electronics design. The internal electronics must be open and exposed to allow charging cables to connect. These ports put a limitation of how shock, dust, and waterproof devices can be.

However, what if devices could charge automatically without a need for ports or charging cables? This possibility has been explored with inductive charging pads. Inductive chargers offer high efficiency, but the transmitting and receiving coils need to be equally sized and oriented such that all the magnetic flux transmitted must be received. Such pads solve the problem of relying on cables and connectors, but the limited range of only a few centimeters and stringent orientation requirements mean that this technology can only be used while the device is stationary and thus batteries still need to be large and abundant.

J. D. Scharf from Plainview, NY (e-mail: jdscharf@umass.edu).
S. Pietryka from Sandwich, MA (e-mail: srpietry@umass.edu).
S. Bevacqua from Falmouth, MA (e-mail: sbevacqu@umass.edu).

Magnetic Resonant Coils offer a mid range, yet still efficient solution to this problem. The transmitting and receiving coils resonate at a fixed frequency, resulting in a high quality factor. This quality factor makes up for the fact that the coils have a lower coupling factor due to increased ranges and non-ideal relative coil orientations. The resonant fields can also charge multiple devices at once without requiring direct line of sight to the receiving devices. Ranges of two meters have been successfully demonstrated, meaning this technology could in the future be used to directly power devices or charge devices as one moves around, resulting in a diminished need for batteries [2].

This technology has important applications other than consumer electronics. This technology could revolutionize medical implants since the devices could be charged wirelessly from outside the body, instead of requiring invasive surgeries to replace batteries. It also has applications in the transportation industry as electric vehicles become more popular. Charging coils can be embedded in parking lots, bus stops, and even the road to charge vehicles at all times, effectively increasing the range and up-time of these vehicles. Since this technology is still primarily a research topic, the modest application of charging a mobile phone was chosen. The solution will involve a transmitter that will be mounted to the bottom of a desk and will be able to supply power to the receiving coil, located in a phone case, 1 cm above the desk and 1cm below the desk. The iPhone 4 will be utilized, placing a limit on the size of the receiving coil to a maximum of 10.5 cm by 5.86 cm. The transmitting coil has no size restrictions. The input power will be limited by the standard wall output of 120 VAC at 60 Hz. The maximum allowed electric and magnetic fields are determined by the IEEE [3]. The specifications are listed in Table 1.

Table 1: Specifications

System Input	120 VAC at 60Hz
Resonant Frequency	6.78 MHz
Distance/Range of Energy Transfer	1 cm
Minimum Output Power at Receiver	2.5W
Minimum Total System Efficiency	≥10%

II. Design

A. Overview

The design for the magnetic resonant wireless phone charger can be broken into two main blocks with several subsystems each, which are illustrated in the block diagram below in Figure 1. The first major subsystem is the transmitter that

consists of a power supply, an oscillator, an amplifier, impedance matching network, and a resonant coil. The transmitter coil and circuitry are enclosed within a plastic case that can be attached underneath a desk or any other location desired by the user. The receiver consists of a resonant coil, an impedance matching network, a rectifier, and voltage regulator. A phone case will be 3D printed and the receiver coil and circuitry will be placed inside. A small USB cable will then connect the phone to the output of the voltage regulator to charge the phone. Additionally, there is also the option to include a repeater located at some point between the transmitter and receiver. A repeater is another coil that is tuned to the same resonant frequency as the transmitter and receiver coils, which can help to improve distance and efficiency of the power transfer [4]. However, we did not use a repeater in the final design.

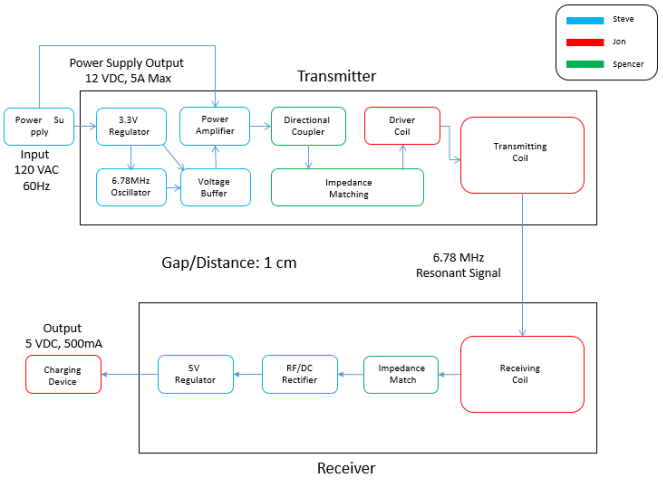

Figure 1. Block Diagram

The block diagram shows the subsections of the two major blocks used for the phone charger as well as division of labor among the team. The following descriptions outline each subsection as well as the technology used to create and test them before implementation.

B. *Power Supply*

A power supply or AC/DC converter is the first step in the block diagram because it is used to power the oscillator, voltage buffer, and power amplifier on the transmitter. AC power directly from the wall operates around 50-60 Hz, which is much lower than the resonant frequency of the coils. Instead of directly converting the frequency from 60 Hz to 6.78 MHz, the AC wall power will be converted to DC with the power supply and then used to power the oscillator at the resonant frequency of the coils. To meet the 10 percent efficiency specification at the maximum distance while supplying 2.5 W to the phone, the required power supply will need to be able to source at least ten times the output power. Therefore, we selected a 60W computer power supply, CUI Inc. ETSA 60W UD [5]. The power supply converts the 120VAC input to a 12V output at 5A maximum. The supply output was selected based on the operating voltage of the power amplifier at about 12V. The oscillator and voltage buffer use lower voltages, which were achieved using a switching voltage regulator.

C. *Switching Voltage Regulators*

On the transmitter, the oscillator and voltage buffer require a supply voltage that is less than the output of the wall power supply. The two ICs have an overlapping supply voltage of 3.3V, so a voltage regulator was used to convert the 12V power supply output to 3.3V. The voltage regulator on the transmitter is Texas Instruments' LM2594N-3.3, which can take a 4.5V-40V input and produce an output of 3.3V at 500mA maximum [6].

Another voltage regulator was used on the receiver to convert the unregulated DC signal from the rectifier to the proper voltage for USB charging. We used a Texas Instruments' LM2575T-5.0 that accepts a 4V-40V input and has a 5V output at up to 1A [7]. The wide input voltage range is important because the rectified signal on the receiver varies as the distance between the transmitter and receiver coils changes. Additionally, both voltage regulators used are switching regulators because they have improved efficiency over linear regulators.

D. *Oscillator*

Nearly every circuit contains an oscillator of some type to control the frequency of operation. In this case, the oscillator is used to set the resonant frequency of the transmitter and receiver coils. There are a wide variety of oscillators that can produce frequencies in the megahertz range, but after experimenting with some, such as the Colpitts oscillator, we settled on a quartz crystal oscillator. The oscillator we selected was an Epson SG-210STF 6.7800ML crystal oscillator [8]. We used a crystal oscillator because the frequency of the output signal remains much more stable than an LC oscillator. The output of the oscillator was a square wave consistently at 6.78MHz, which can be seen in Figure 2. The square wave is later converted to a sine wave in order to remove the additional harmonics of our resonant frequency. The oscillator output is then put into a voltage buffer to prevent loading from the power amplifier.

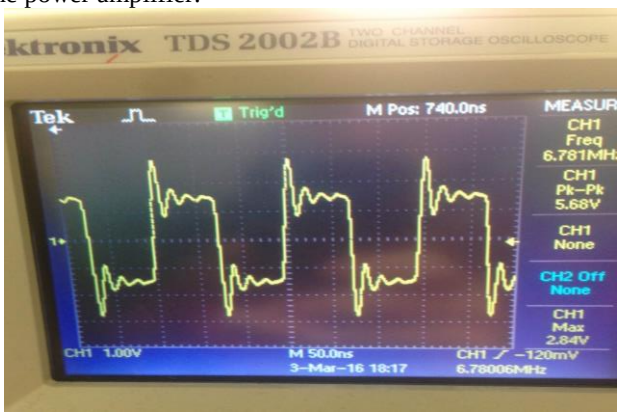

Figure 2. Oscillator output signal

E. Voltage Buffer

As mentioned above in the oscillator section, operating at the resonant frequency is crucial for the technology to work optimally. By loading the output of the oscillator, the frequency can shift away from resonance or even attenuate the oscillating signal. To prevent this from happening, a voltage buffer is placed at the output of the oscillator before the power amplifier. Typical op amp ICs can be configured to a buffer where the gain is close to 1, however because we are operating at a high frequency, a buffer amplifier with a higher bandwidth was chosen. The selected buffer is the Texas Instruments BUF634P, which has an option for up to 180MHz 3dB bandwidth [9]. Additionally, the slew rate limit of the buffer changes the square wave from the oscillator to a triangular waveform. Although a slew rate limit is usually yields poor results, it seems to have been a benefit for our application. Finally, before the output signal is fed to the power amplifier, it is passed through a resistive voltage divider to change the input power to the amplifier.

F. Power Amplifier

Once the 6.78MHz signal is produced and buffered, it needs to be amplified so that a considerable amount of power can be transmitted at the resonant frequency. However, many high frequency power amplifiers are expensive and outside of our $500 budget. Additionally, designing efficient amplifiers can be costly in time, so we found a ham radio transceiver amplifier from an independent manufacturer on eBay [10]. The amplifier contains a preamplifier stage, an RF driver stage, and a final output power stage. A photo of the amplifier can be seen in Figure 3. With a supply voltage up to 14V and an input of 1-5mW from 3-30MHz, approximately 40dB of gain can be achieved. We approximate about a 1mW input signal, which would indicate about 10W output of RF power. However, we do not know this for sure because even though the voltage of the 6.78MHz signal is known, the phase remains unknown. We tried using the power meter in the Microwave Instructional Laboratory, but the probe is not rated for frequencies lower than 15MHz. As a result, we obtained power measurements that were not accurate. The input and output of the amplifier require SMA connectors with an impedance of 50 ohms. The low input resistance would result in loading the oscillator signal if the buffer was not present. The output of the amplifier is fed to a simple third order Butterworth low pass filter with a cutoff frequency of 13.56MHz matched to 50 ohms. After the filter, the output goes to the bi-directional coupler.

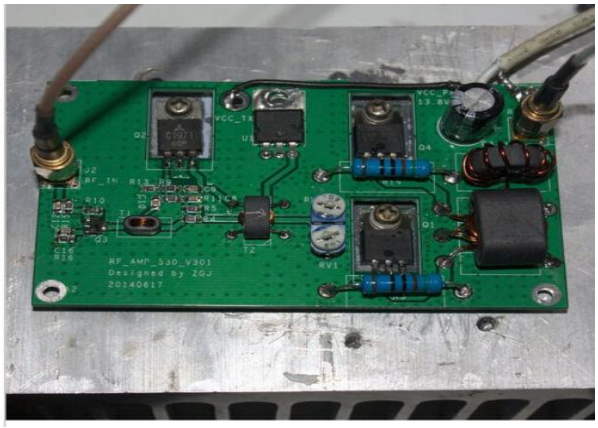

Figure 3. Power amplifier

G. Directional Coupler

The original intent of this block was to use a bi-directional coupler to measure incident and reflected power from the power amplifier into the transmitting coil. The coupled outputs would then be fed into an IC in order to quantify any impedance mismatch and inform an adaptive impedance matching network. The Mini-Circuits SYDC-20-31HP+ Surface Mount Directional Coupler was chosen for this task [11]. It was chosen for a few key reasons. It operates in the frequency band of 1.5 to 30 MHz, so our 6.78 MHz signal could be properly measured. It has a high power handling capability of 50 W, so even if we had to make up for inefficiency in the wireless transfer, we could compensate with more power from the amplifier. It also boasts a high (33 dB) directivity, low (0.1 dB) mainline loss, and a high (38 dB) return loss. This means that the coupler would not dissipate much of the incident power, lowering our overall efficiency, and would provide accurate measures of the incident and reflected waves while sinking reflections to protect the power amplifier. As will be explained in the Impedance Matching Networks section, the adaptive impedance matching network was scrapped. The coupler was repurposed as a circulator with the coupled ports terminated in matched 51 ohm loads. A circulator allows signals to pass in one direction but not the other. It passes the input to the thru port with little loss and sinks any reflections coming back to the coupler to ground. Signals coming into the thru port will not be passed to the input port and signals coming from the ground will not be passed to the thru port. So the coupler is simply used to sink reflections to keep them from damaging the amplifier. Its inclusion significantly lowered the rate at which the power amplifier heated up, indicating its effectiveness.

H. Impedance Matching Networks

Magnetic resonant wireless power transfer involves creating an LC resonance and transferring power via electromagnetic coupling. As a result, the magnetic coupling can be illustrated by the mutual inductance, L_m, shown in Figure 4 [12], where Z_{source} is the characteristic impedance, Z_{load} is the impedance of the load, and the ohm loss due to radiation is represented by R.

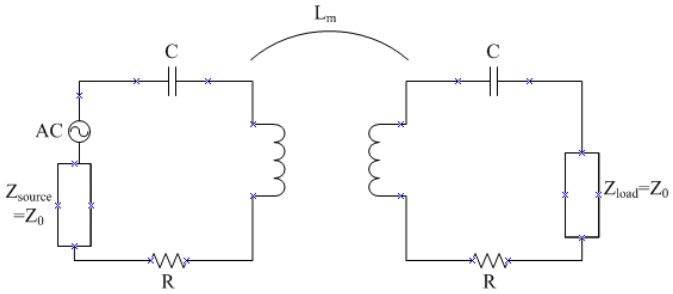

Figure 4. Transmitter and Receiver Schematic

In order to achieve efficient wireless resonant power transfer for our system, both the transmitter and the receiver coils need to be operating at resonant frequency. From this topology, the resonance frequency can be calculated based on the following component values. In order to satisfy the resonance condition the reactance must be zero as shown in equation (1) below. Following this, the two resonant frequencies for both the transmitter and receiver can be calculated from equations (2) and (3). Next, the two resonant frequencies can be used to calculate the coupling coefficient shown in equation (4).

$$\omega_m = \frac{\omega_0}{\sqrt{(1+k)}} = \frac{1}{\sqrt{(L+L_m)C}} \quad (1)$$

$$\omega_m = \frac{\omega_0}{\sqrt{(1+k)}} = \frac{1}{\sqrt{(L+L_m)C}} \quad (2)$$

$$\omega_e = \frac{\omega_0}{\sqrt{(1-k)}} = \frac{1}{\sqrt{(L-L_m)C}} \quad (3)$$

$$k = \frac{L_m}{L} = \frac{\omega_e^2 - \omega_m^2}{\omega_e^2 + \omega_m^2} \quad (4)$$

However, as the distance between the coils increases, the coupling between the two coils weakens and the coupling coefficient that ensures efficient power transfer reduces. As a result, the impedance for both the transmitter and receiver circuits will change due to the change in the coupling coefficient, and the effective resonance frequency will change as well. **[**12**]** Shows how the coupling factor reduces with increasing distance [Figure 5] for two 5 turn, 150 mm radius, and 5 mm pitch helical coils.

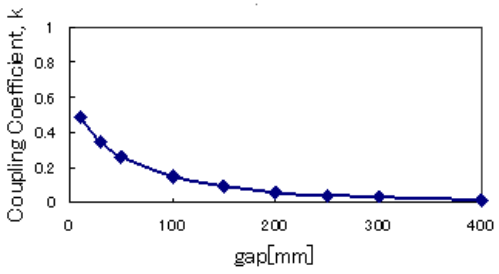

Figure 5. Coupling Factor vs. Distance between Coils

As a result, the efficiency vs. frequency for increasing distances can be seen in Figure 6 from article [12**]**, where the pink curves represent the power efficiency of reflection and the blue curve represents the power efficiency of transmission.

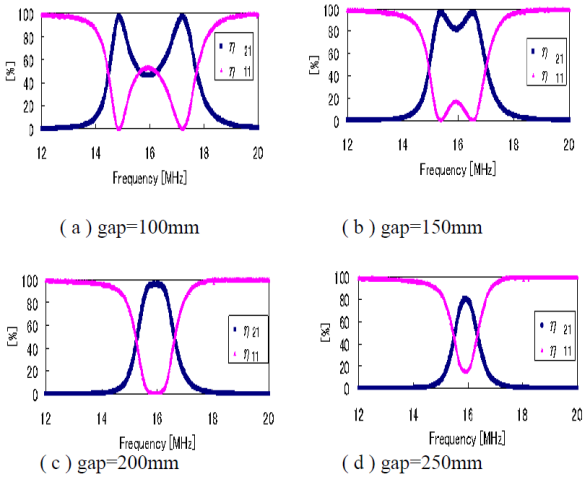

Figure 6. Efficiency vs. Frequency at Various Gap Distances

From the figure one can see that at a shorter distance of about 100 mm, there are two twin peaks in efficiency but as the distance increases these frequencies converge at a midpoint and eventually reduces in amplitude.

Due to the change in resonant frequency with distance, prior research has demonstrated wideband frequency tuning techniques that can automatically change the operating frequency to the resonant frequency at various distances to ensure optimum efficiency. However, due the Industrial-Scientific-Medical (ISM) band regulations, there are only certain frequencies allocated with a limited bandwidth available for purposes other than for communication. In the Code of Federal Regulations, Tile 47, Part 15, available operating frequencies are specified in Table II with the corresponding bandwidths. From the Figure 7 [13], it is illustrated that at lower frequencies there is considerable power loss, and at higher frequencies beyond 20 megahertz, there arises major design problems due to cost, size, and power allocation for certain components. As a result, it was found that the best operational frequency is a stable 6.78 megahertz, which has a practical bandwidth of 15 kilohertz.

ISM frequency	Tolerance
6.78 MHz	±15.0 kHz
13.56 MHz	±7.0 kHz
27.12 MHz	±163.0 kHz
40.68 MHz	±20.0 kHz
915 MHz	±13.0 MHz
2,450 MHz	±50.0 MHz
5,800 MHz	±75.0 MHz
24,125 MHz	±125.0 MHz
61.25 GHz	±250.0 MHz
122.50 GHz	±500.0 MHz
245.00 GHz	±1.0 GHz

Table II. Code of Federal Regulations, Tile 47, Part 15 Available ISM Band Frequencies

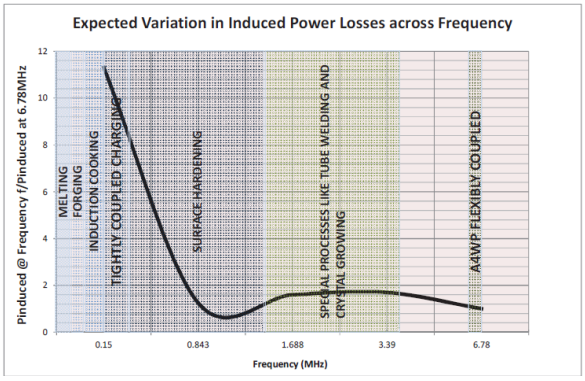

Figure 7. Power Loss vs. Operational Frequency

Therefore, in order to ensure that we are performing at resonant frequency without violating ISM band regulations and changing our operational frequency, impedance matching can be used to obtain the optimum wireless power transfer efficiencies at various distances. From article [12], Figure 8a illustrates that at their operating frequency of 13.56 megahertz, before impedance matching that obtained about a 50% efficiency wireless power transfer. However, Figure 8b shows that after impedance matching, they were able to operate at resonant frequency obtaining a wireless power transfer efficiency of 90%.

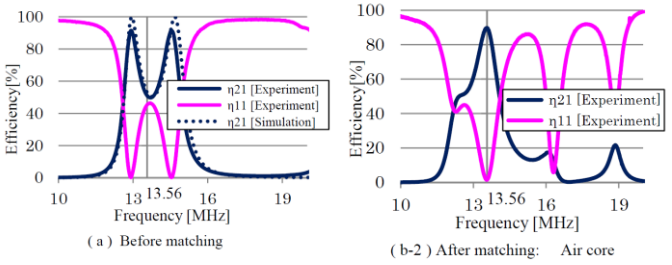

Figure 8. Efficiency vs. Frequency After and Before Impedance Matching

In developing an impedance matching network suitable for achieving optimum efficiency, it is found that a pi-model typology is strongly preferred over other types of networks, Figure 9 [14]. Unlike an L-model typology, a pi-model typology enables wideband impedance matching to load impedances that are greater than, equal to, or less than the source impedance.

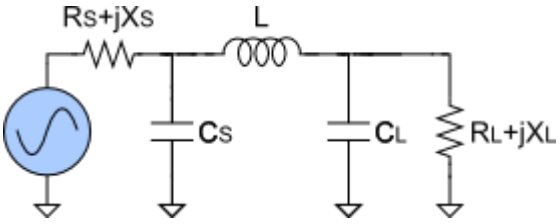

Figure 9. Pi-Model Impedance Matching Network

To determine the proper values for the impedance matching network, a vector network analyzer, or VNA, was used to measure the complex input impedance of our system of driver coil, transmitter coil, and receiver block. Figure 10 shows the Smith Chart of this input impedance across the frequency range of 300 kHz –15 MHz. At our particular frequency of 6.78 MHz, Z_{in} = 75.3 –j848 ohms. Using the following equation (5) and matching to the 50 ohm output of the coupler,

$$Z_{input} = \left(\left((R_L + jX_L) \,//\, \left(\frac{1}{j\omega \cdot C_L}\right)\right) + j\omega \cdot L\right) \,//\, \left(\frac{1}{j \cdot \omega \cdot C_s}\right) \quad (5)$$

the component values of Cs = 1.11 nF, L = 6.7 uH, and Cl = 60 pF were selected and implemented with fixed lumped elements. Before implementing the matching network, a VSWR of 11 was measured with the VNA at our frequency of operation. With the matching network in place, a VSWR of 2 was measured, so while the match is not perfect, the network significantly improves the performance of our system. We also encountered problems with heat dissipation in the matching network. Since it is implemented after the power amplifier, this block is exposed to high voltage and current so the inductor heated up significantly, changing its inductance. The changing inductance causes more reflections, causing the coupler and other components to heat up more increasing loss and lowering efficiency in our system. We addressed this issue by including a 12 Vdc fan in the packaging of our transmitter to cool these components.

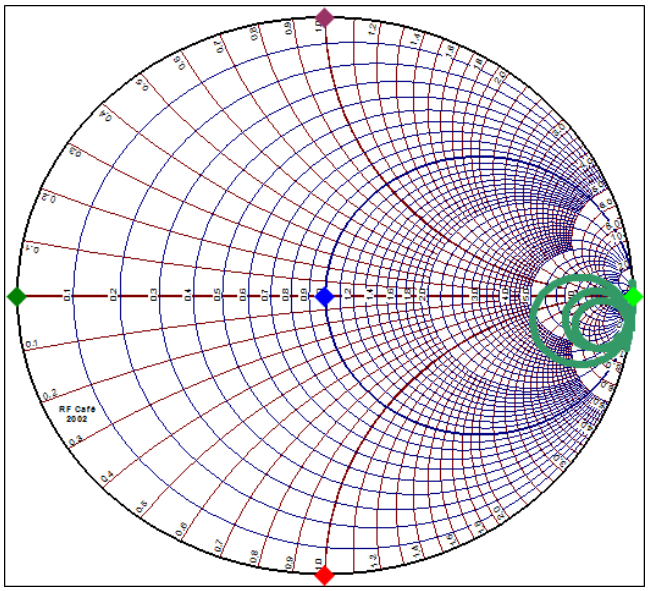

Figure 10. S_{11} Looking into Driver Coil

To further improve the matching in our system, an adaptive impedance matching network could be implemented. Such a network would use variable capacitors to tune the matching network in real time. We planned on building one but were stopped by technological, cost, and time constraints. Most adaptive matching networks are implemented using varactor diodes, or varactors. Varactors work by applying a reverse bias voltage to vary and control the junction capacitance. This was not feasible in our application because the power amplifier was creating a signal in excess of 60 Vpp, so any bias voltage we could output from a microcontroller would be completely overwritten by the mainline signal and we would not be able to

control the variable capacitance. Other applications use digitally tunable MEMS capacitors. They are ICs with a digital input line that controls an array of capacitors in the chip that can be connected in various ways to change capacitance. However they can only stand voltages on the order of 5-10 volts across its capacitive output, making them unfit for our system. High power transmitting systems use vacuum variable capacitors which operate by actuating a piston inside of a vacuum to vary capacitance. Such devices were far outside of our budget. The only feasible solution was a mechanically tunable parallel plate capacitor. In order to implement it we would have had to design and create a motorized capacitor utilizing a stepper motor and microcontroller. Unfortunately we didn't have the time or budget to implement this, so we stuck with our fixed impedance matching network.

I. Transmitter and Receiver Coils

In designing the transmitter and receiver coils, the most important consideration is the quality factor, Q. The quality factor of the resonant coils is a measure of how well the coils store and dissipate energy. Essentially, the higher the quality factor, the more efficient the coils are in storing energy.

Calculating the quality factor is illustrated in Figure 11 [2]. From the quality factor, the figure of merit, U, can be determined. Accordingly, by assuming an optimum impedance matching network, the optimum power efficiency vs. figure of merit is illustrated in Figure 11, and the relationship shows that a large figure of merit will lead to a more efficient power transfer. Since the figure of merit is determined by the coupling coefficient and the quality factor of the two coils, increasing the quality factor will increase the optimum wireless transfer efficiency.

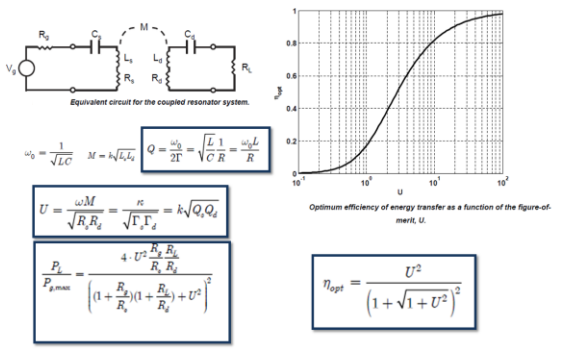

Figure 11. Quality Factor and Figure of Merit Calculations

The quality factor is dependent on the angular frequency, inductance, and resistance. Since the frequency will be fixed at 6.78 megahertz, having the smallest coil resistance and largest inductance will lead to the highest quality factor. The inductance and resistance of a coil can be calculated from the equations in Figure 12 [15]. The equations show that the inductance has a relationship to the number turns, N, squared, while the resistance is only linearly dependent. As a result, the Q increases linearly with the number of turns in a flat coil design.

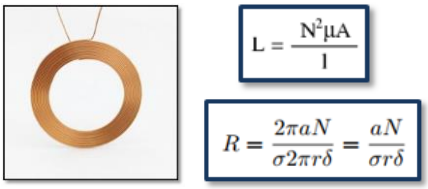

Figure 12. Calculations for Inductance and Resistance for Flat Coil Design

Apart from the quality factor, the ratio of the coil sizes also considerably affects the wireless transfer efficiency. Figure 13 illustrates that as the distance in relation to the transmitting coil diameter increases, different coil ratios will lead to different efficiencies [16]. For instance, when the ratio of the receiver coil diameter to the transmitter coil is 1, the maximum wireless transfer efficiency is observed. However, the smaller the ratio becomes, the quicker the efficiency tends to drop off. At about a ratio of .3, the efficiency is about 60% at 1 transmitter coil length. As a result, in order to meet wireless power transfer efficiency above 40% at a coil length distance, a ratio above 0.3 should be used.

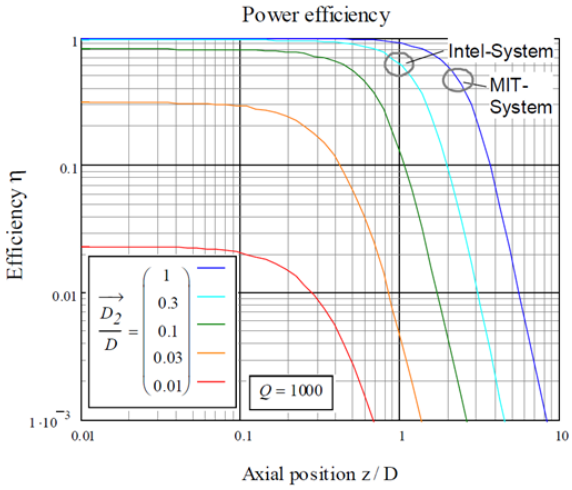

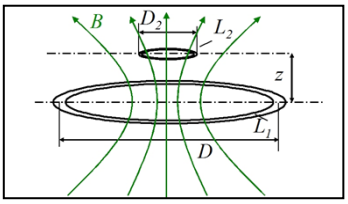

Figure 13. Plot When Quality Factor is 1000 of Different Ratios at of Receiver Coil Diameter to Transmitter Coil Diameter in Efficiency vs. Distance per Receiver Coil

In Figure 14, the Q factor for the two coils is 1000. However, if this Q factor were to increase, the efficiency drop would extend beyond what is shown in the diagram. In other words, the higher the Q factor, the smaller the ratio can be made for the same amount efficiency.

In designing the coils, a multi-turn transmitter and receiver topology should be implemented with the largest wire

thickness possible for the fitted area to obtain a smaller resistance. Additionally, a receiver to transmitter diameter coil ratio should be greater than 0.3 to ensure that the efficiency doesn't drop off considerably at shorter distances. To test the quality factor of the coils, an LCR parameter analyzer is used.

The receiver coil diameter and size is limited to the area of the phone or the phone case (Figure 14). As a result, the transmitter coil diameter is limited to approximately 175 mm or approximately three times the width of the phone when taking into account the efficiency drop off from the ratio of receiver sizes mentioned in [16] and shown in Figure 12.

Figure 14. Dimensions for standard IPhone 4

In order to maximize the Q-factor for both the transmitter and receiver coils for their respective sizes, simulations were performed for the optimal number of turns, wire diameter, and diameter length for the design. Using the equations given from [17] shown in Figure 15, a simulation was performed on the quality factor's dependence on the key parameters mentioned previously.

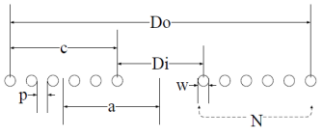

Fig. 1. Cross-sectional view of flat spiral coil.

$$L(H) = \frac{N^2(D_o - N(w+p))^2}{16D_o + 28N(w+p)} \times \frac{39.37}{10^6} \quad (3)$$

$$R_{DC} = \frac{l}{\sigma\pi(w/2)^2}, \quad \delta = \frac{1}{\sqrt{\pi f\sigma\mu_o}} \quad (5)$$

$$R = R_{DC}\frac{w}{4\delta} = \sqrt{\frac{f\pi\mu_o}{\sigma}}\frac{N(D_o - N(w+p))}{w} \quad (6)$$

$$D_i = D_o - 2N(w+p), \qquad l = \frac{1}{2}N\pi(D_o + D_i) \qquad Q = \frac{1}{R}\sqrt{\frac{L}{C}} = \frac{39.37}{10^6}\sqrt{\frac{f\pi\sigma}{\mu_o}}\frac{wN(D_o - N(w+p))}{8D_o + 14N(w+p)} \quad (7)$$

$$a = \frac{1}{4}(D_o + D_i), \qquad c = \frac{1}{2}(D_o - D_i) \quad (2)$$

Figure 15. Computational model and equations of spiral coil based on various parameters, where:
N is the number of turns, D_0 is the outer diameter, p is the spacing between turns, w is the wire diameter, D_i is the inner diameter, l is the total wire length, α is the winding radius, c is the radial depth, and f is the resonant frequency

After simulation, it was found that for the frequency and turn spacing, the effects on the quality factor are fairly linear, in that in order to get the highest quality factor, one would want a higher frequency and a smaller spacing between the wires. Therefore, the following three 3D graphs in Figure 16 were created to optimize the number of turns, outer diameter size, and wire diameter for the transmitter coil.

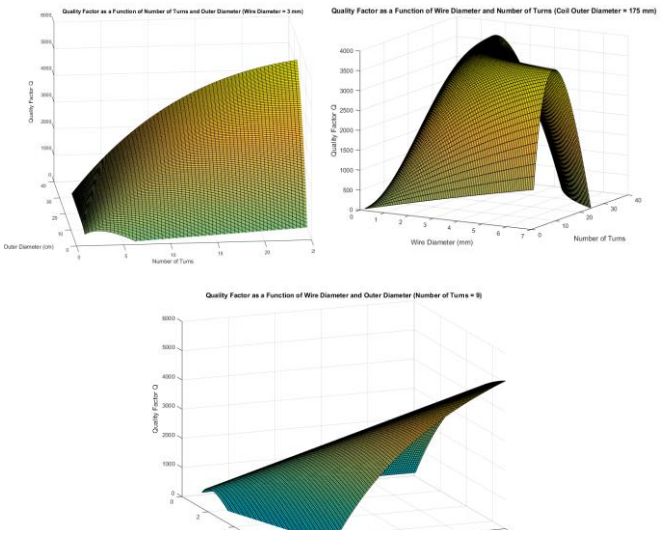

Figure 16. MATLAB Simulation plots

In addition to the quality factor, a simulation was also performed for the coupling coefficient from [18]. From the resulting MATLAB plot from Figure 17, it can be see that the coupling coefficient with respect to distance matches well with the theory of drop off in coupling over distance.

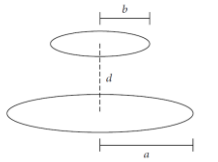

FIGURE 2: Two coaxial coils with radii a and b.

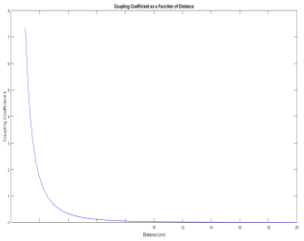

$$M = \frac{\mu\pi n_1 n_2 a^2 b^2}{\sqrt{(a+b)^2 + d^2}\left[(a-b)^2 + d^2\right]} \quad (14) \qquad k = \frac{M}{\sqrt{L_i L_j}}$$

Figure 16. Equations and MATLAB Simulation for Calculating Coupling Coefficient

From these plots, the transmitting coil was designed, such that the maximum quality factor was achieved. From Figure 18, it can be seen the values predicted matched closely with the values calculated, although the Q-factor was over estimated since the equations did not take into account the parabolic nature of the quality factor with frequency. However, the parameters, L and R, were optimized, which is what results in a high magnitude quality factor.

Picked Values for Transmitting Coil

- D_0 = 175mm
- w = 2.05 mm (12AWG)
- N = 23 turns
- s = As close to zero as possible

Theoretical Values:
C = 6.602 pF L= 83.233 uH
R (AC) = .9440 ohms
Q_Factor (6.78 Mhz) = 3544

Measured Values:
C = assumed 0 F L = 61.5 uH
R(AC) = .51 ohms
Transmitter Q Factor = 349

Figure 18. Parameters and Measurements for Transmitter Coil Design

However, from measurements taken from a vector network analyzer, the transmitter coil's parasitic capacitance turned out to be fairly significant, in that at our resonant frequency (6.78 MHz), the coil was capacitive rather than inductive. As a result, in order to tune the transmitter coil to resonate at our specified frequency, a series inductance and capacitance was added in a small network to tune the overall resonant frequency of the circuit. This is done by adding reactive and real impedance values in series to cancel out the excess reactive component of the transmitter coil caused by the parasitic capacitance.

The MATLAB simulation calculations were also used to obtain the dimensions for the receiver coil shown in Figure 19.

Picked Values for Receiver Coil

- D_0 = 70 mm
- w = 2.05 mm (12AWG)
- N = 10 turns
- s = Close to zero

@6.78 MHz :
Receiver Q Factor = 210.2

Experimental Values at Resonance

- L = 4.5 uH
- R = .1422

Figure 19. Parameters and Measurements for Receiver Coil Design

As one can see from Figure 18 and 19, the quality factor of the coils designed were fairly large compared to the typical value of Q = 100 that is offered by most commercially available coils.

J. Driver Coil

Due to the high quality factor of the receiver coil, the values needed to impedance match from the 50 Ω output load of the amplifier to the low real impedance of the transmitter coil is too small for the tolerances of lumped element components. In other words, a high quality factor was prioritized, but the coils were difficult to integrate with the rest of the system.

To remedy this issue, a driver coil was designed and created to have a higher real impedance so that the amplifier could be better matched with reasonable component values. In integration, the driver coil is connected to the impedance matching network coming out of the driver and is inductively coupled to the transmitter coil, so that power is distributed like a transformer (As shown in Figure 20 taken from [19]). This ensures that the high real impedance of the driver coil allows one to better impedance match.

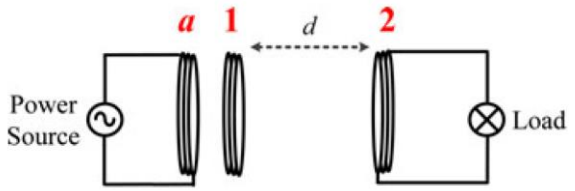

WPT system with an additional resonator at the transmitter side

Figure 20. Schematic of Driver Coil Integration

In addition, the driver coil is serving as a step-down transformer, in which the voltage is stepped down between the inductive coupling and the current is stepped up. This is highly desired since a higher transmitting current creates a larger magnetic field, while a higher voltage creates a higher electric field, which is less desired for our application.

The current step-up factor is determined by the square root of the ratio of the inductances as seen in the equation below:

$$\text{Stepup Factor} = \sqrt{\frac{L_{Driver}}{L_{transmitter}}} \qquad L = \frac{N^2 \mu A}{l}$$

From this equation, one may also see that if the coils designed were helical, in that the inductances were dependent on a factor of N^2, the current step-up factor would be determined by the ratio of the number of turns for the two coils. Therefore, the maximum current step-up factor for two spiral coils can be determined by:

$$\frac{N_{Driver}}{N_{Transmitter}}$$

Using the same equations in [17] for calculating the inductances for spiral coils shown in Figure 15, simulations were performed to optimize the driver coil design for the maximum step-up factor for our transmitting coil. Figure 21 shows a 3D graph of the current step-up factor as a function of the wire diameters for each coil. In this example, the ratio of turns is equal 4.

As one can see, the ratio is maximized when the wire diameter for transmitter coil is significantly less than the wire diameter for driver coil. In this example, when the ratio of wire diameter of transmitting coil to the wire diameter of the driver coil is maximum, the maximum step-up current factor of 4 is achieved.

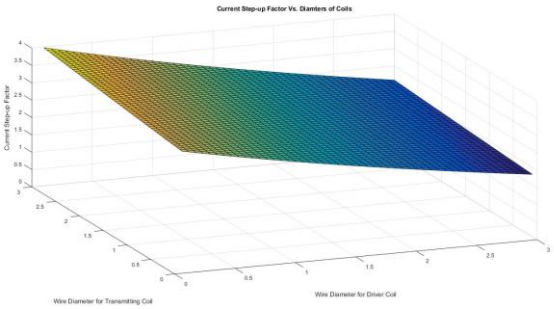

Figure 21. Current Step-Up Factor as a Function of Diameter of

From this information, smaller gauge wire was purchased for the designed driver coil. Figure 22 shows the dimensions and values:

- VNA:
  - 38.38 ohms @ 6.78Mhz
  - Inductance:
  - 18 AWG

~ 58 turns

Diameter = 175 mm

  - Same as transmitter
  - Wire Length= ~20 meters

$$\sqrt{\frac{L_{Driver}}{L_{transmitter}}} = \sqrt{\frac{2.3mH}{62\ \mu H}} = 6.09$$

Figure 22. Dimensions and Values of Driver Coil
(Driver coil is the coil beneath the black transmitter coil)

K. Phone Case and Transmitter Enclosure Design

The phone case was designed in Inventor based on the dimensions of the IPhone shown in Figure 14. Figure 23 shows the phone case, receiver case, lid, and the complete integration designed and modelled in Inventor before being 3D printed in M5 and the final printed case. The phone case was designed to have a separate compartment to house the receive coil behind a case for the phone. The total dimensions were 83 mm by 145mm by 24 mm.

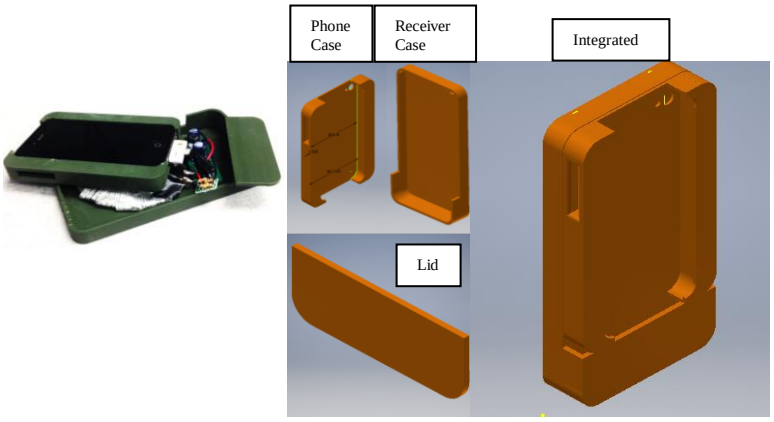

Figure 23. Phone Case Inventor Model and Printed Result

For the case designed shown in Figure 22, the case was made of a plastic material that was tested between the between the coils during operation to ensure power could be transferred between material. In addition the case also had a drop down opening for the amplifier heat sink shown in Figure 24, so that the transmitter could still be mounted under a desk with a flat surface.

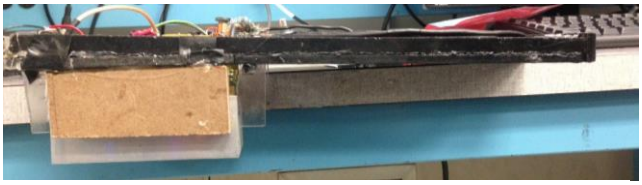

Figure 24. Side-view of Enclosed Transmitter Circuitry

L. RF/DC Rectifier

A rectifier is important in the receiver section because it converts the received signal at 6.78 MHz back to a DC voltage that can be utilized by electronics, such as the cell phone. We used a bridge rectifier consisting of Schottky diodes. Schottky diodes have a smaller forward voltage and therefore rectify the signal faster without a significant voltage drop. The output of the rectifier has ranged from 8-14VDC depending on the distance between the transmitter and receiver coils. The DC output is then converted to a 5V output from the switching voltage regulator discussed in part C.

III. PROJECT MANAGEMENT

After MDR, the group focused on the tasks assigned on the Gantt chart from the MDR report in order to complete the project. However, some tasks were shifted between members so that more focus could be put on other aspects of the project. For example, after determining that a tunable impedance matching network was outside of our budget, Spencer took over Jon's role of the impedance matching network. This allowed Jon to begin designing the 3D printed phone case and

constructing the housing for the transmitter. Besides these task changes, everything else remained the same. Steven Bevacqua worked on integrating the power supply, oscillator, buffer, and amplifier on the transmitter as well as the rectifier and regulator on the receiver. Spencer Pietryka changed the bidirectional coupler to a circulator for added protection on the amplifier, created new impedance matching networks, and took VNA measurements to facilitate the impedance matching. Jonathan Scharf finalized the coil designs and created the housings for the transmitter and receiver phone case. Finally, we continued to meet weekly with our advisor, Professor Aksamija, who helped us prioritize the order of tasks to be completed as well as help us think of general solutions for problems that arose.

IV. Conclusion

At the time of MDR, our physical project demonstrated a proof of concept, showing that it was feasible to transmit and receive power at longer ranges than current inductive technology using a function generator, large coils, and LEDs. Since MDR, we have completely constructed the project in its current form.

A DC power supply takes in a $120V_{AC}$, 60Hz signal from the wall outlet and outputs a 12 V_{DC} signal. This voltage is used by the power amplifier, cooling fan, and voltage regulator that creates a 3.3 V_{DC} voltage. This voltage is used by the oscillator and voltage buffer to create a stable 6.78 MHz signal. That signal is input to a power amplifier which then outputs to the coupler, functioning as a circulator. The output of the circulator is impedance matched to a driver coil which inductively couples the signal to a transmitting coil. The receiver coil intercepts the magnetic field of the transmitter and the created current is rectified, regulated, and then outputted to the USB interface of the iPhone 4. All of these subsystems have been designed and integrated since MDR.

Our final project was able to accomplish our goal of charging a phone, successfully delivering at least 2.5 W across a range of 1 cm while operating within the 6.78 MHz ISM band. The most significant problem was matching the impedance of the coils to the 50 ohm output of the amplifier and coupler in order to reduce reflections, and in order to achieve better results, the system would need further optimization.

Appendix

A. Cost

The total cost of our system assumes the consumer already has an iPhone 4. Also there was no cost break on the amplifier since it was ordered from eBay.

Table III. Cost Breakdown

Item	Quantity	Prototype Price	1000 Unit Price
Coupler	1	$ 39.95	$ 32.95
6.8 uH Inductor	1	$ 0.59	$ 0.47
2.2 pF Capacitor	3	$ 0.29	$ 0.07
10 pF Capacitor	5	$ 0.20	$ 0.04
68 pF Capacitor	1	$ 0.25	$ 0.05
5 pF Capacitor	1	$ 0.49	$ 0.14
330 nH Inductor	1	$ 0.49	$ 0.22
1 uF Capacitor	1	$ 0.40	$ 0.11
51 ohm Resistors	2	$ 0.10	$ 0.01
75 kohm Resistor	1	$ 0.10	$ 0.01
43.2 kohm Resistor	1	$ 0.10	$ 0.01
49 kohm Resistor	2	$ 0.10	$ 0.01
Power Supply	1	$ 23.94	$ 19.59
3.3 Reg	1	$ 2.86	$ 1.42
Buffer	1	$ 8.63	$ 4.53
Oscillator	1	$ 1.79	$ 1.44
Amplifier	1	$ 45.92	$ 45.92
5V reg	1	$ 2.89	$ 1.42
Power Conn	1	$ 1.12	$ 0.47
Fan	1	$ 5.07	$ 2.90
Coil Wire	1	$ 36.00	$ 8.40
Case Materials	1	$5	$ 1.00
TOTAL		$ 176.28	$ 121.19

References

[1] C. X. Zu and H. Li, “Thermodynamic analysis on energy densities of batteries,” Energy Environ. Sci., 2011, vol. 4, pp. 2614-2624

[2] M. Kesler, "Highly resonant wireless power transfer: safe, efficient, and over distance.", WiTricity Corporation. 2013.

[3] “IEEE Standard for Safety Levels with Respect to Human Exposure to Radio Frequency Electromagnetic Fields, 3 kHz to 300 GHz”, IEEE Std. C95.1-2005.

[4] Dukju Ahn; Songcheol Hong, "A Study on Magnetic Field Repeater in Wireless Power Transfer," in Industrial Electronics, IEEE Transactions on , vol.60, no.1, pp.360-371, Jan. 2013

[5] CUI Inc., “AC-DC Power Supply,” ETSA 60W UD datasheet, Nov. 2014.

[6] Texas Instruments, “LM2594/LM2594HV Simple Switcher Power Converter 150kHz 0.5A Step-Down Voltage Regulator,” Dec. 1999 [Revised Apr. 2013].

[7] Texas Instruments, “LM1575/LM2575/LM3575HV Simple Switcher 1A Step-Down Voltage Regulator,” May. 1999 [Revised Apr. 2013].

[8] Seiko Epson Corporation, “Crystal Oscillator (SPXO),” SG-210 STF datasheet.

[9] Texas Instruments, “BUF634 250-mA High-Speed Buffer,” Sept. 2000 [Revised Nov. 2015].

[10] "Assembled Finished 45W ssb linear power amplifier for transceiver HF radio AMP", *eBay*, 2016. [Online]. Available: http://www.ebay.com/itm/Assembled-Finished-45W-ssb-linear-power-amplifier-for-transceiver-HF-radio-AMP-/121960051022. [Accessed: 28- Apr- 2016].

[11] Mini-Circuits, “Surface Mount Directional Coupler,” SYDC-20-31HP+ datasheet, 2016

[12] Teck Chuan Beh; Imura, T.; Kato, M.; Hori, Y., "Basic study of improving efficiency of wireless power transfer via magnetic resonance coupling based on impedance matching," in Industrial Electronics

(ISIE), 2010 IEEE International Symposium on , vol., no., pp.2011-2016, 4-7 July 2010

[13] Tseng, R.; von Novak, B.; Shevde, S.; Grajski, K.A., "Introduction to the alliance for wireless power loosely-coupled wireless power transfer system specification version 1.0," in Wireless Power Transfer (WPT), 2013 IEEE , vol., no., pp.79-83, 15-16 May 2013

[14] Aspen Labs LLC, "Pi-Match Impedance Matching Circuit." EEWeb, 2016.

[15] Cannon, B.L.; Hoburg, J.F.; Stancil, D.D.; Goldstein, S.C., "Magnetic Resonant Coupling As a Potential Means for Wireless Power Transfer to Multiple Small Receivers," in Power Electronics, IEEE Transactions on , vol.24, no.7, pp.1819-1825, July 2009

[16] Waters, Benjamin H., Alanson P. Sample, and Joshua R. Smith. "Adaptive impedance matching for magnetically coupled resonators." PIERS Proc(2012): 694-701.

[17] Waters, Benjamin H., Brody J. Mahoney, Gunbok Lee, and Joshua R. Smith. "Optimal coil size ratios for wireless power transfer applications." In Circuits and Systems (ISCAS), 2014 IEEE International Symposium on, pp. 2045-2048. IEEE, 2014.

[18] Mendes Duarte, Rafael, and Gordana Klaric Felic. "Analysis of the Coupling Coefficient in Inductive Energy Transfer Systems." Active and Passive Electronic Components 2014 (2014).

[19] Zhong, W. X., Chenghui Zhang, Xun Liu, and Shu Yuen Ron Hui. "A methodology for making a three-coil wireless power transfer system more energy efficient than a two-coil counterpart for extended transfer distance." Power Electronics, IEEE Transactions on 30, no. 2 (2015): 933-942.